ACS OMEGA

http://pubs.acs.org/journal/acsodf

Article

Anticancer Biosurfactant-Loaded PLA−PEG Nanoparticles Induce Apoptosis in Human MDA-MB-231 Breast Cancer Cells

Aishani Wadhawan, Joga Singh, Himani Sharma, Shristi Handa, Gurpal Singh,* Ravinder Kumar, Ravi Pratap Barnwal, Indu Pal Kaur, and Mary Chatterjee*

Cite This: *ACS Omega* 2022, 7, 5231−5241

Read Online

ACCESS | Metrics & More | Article Recommendations

ABSTRACT: Despite various advancements in cancer therapies, treating cancer efficiently without side effects is still a major concern for researchers. Anticancer drugs from natural sources need to be explored as a replacement for chemo drugs to overcome their limitations. In our previous studies, isolation, characterization, and anticancer properties of a novel biosurfactant from *Candida parapsilosis* were reported. In this study, we report the cytotoxicity of the polymeric nanoparticles of this novel biosurfactant toward breast cancer cells. Biosurfactant-encapsulated polymeric nanoparticles of polylactic acid−poly(ethylene glycol) (PLA−PEG) copolymers were synthesized by the double emulsion solvent evaporation method. Folic acid (FA) was used as a targeting ligand to actively deliver the anticancer cargo to the cancer site. The encapsulation efficiency of nanoparticles was observed as 84.9%, and Fickian diffusion was observed as a kinetic model for the release of biosurfactant from nanoparticles. The controlled delivery of the biosurfactant was noticed when encapsulated in PLA−PEG copolymer nanoparticles. Additionally, it was observed that FA enhanced the uptake and cytotoxicity of biosurfactant-loaded nanoparticles in MDA-MB-231 cancer cells compared to biosurfactant-loaded plain nanoparticles. Induction of apoptosis was observed in cancer cells by these nanoparticles. We explore a potential anticancer agent that can be further analyzed for its efficiency and can be used as an alternative tool.

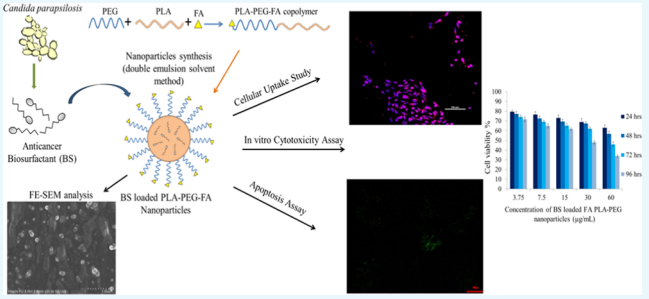

1. INTRODUCTION

Increasing incidence and mortality rates of cancer among people have drawn scientists' attention in the past few decades. Various cancer therapies like physical surgery, chemotherapy, radiotherapy, immunotherapy, and nanotherapy have evolved every decade to overcome this lethal disorder.[1] A major concern of researchers is to treat cancer efficiently without aftereffects. None of the chemotherapeutic drugs are free from side effects. The main problem arises due to their non-specificity and toxicity of drugs as well as their vehicle such as Cremophor EL.[2] In the 1990s, alternative therapies had evolved, such as targeted therapy (kinase inhibitors as therapeutic agents) and immunotherapy (monoclonal antibodies as therapeutic as well as targeting agents).[1] These targeted therapies were observed to impart increased efficiency for the detection and treatment of cancer with reduced side effects. For instance, Koirala et al.[3] evaluated the specificity and toxicity of a folic acid-containing drug delivery vehicle (DDV) in a hepatocellular carcinoma (HCC) model. Their study suggested that PEG incorporation and folate targeting can be used as an efficient strategy for targeted delivery in HCC therapy. Similarly, Law et al.[4] observed that Celastrol—a traditional Chinese medicine used for treating cancer—has poor tumor selection. Therefore, they prepared folate receptor-targeted celastrol AuNP (FCA). It was observed that the delivery of the drug using FCA showed more significant apoptosis than the celastrol AuNP and celastrol alone in both 2D and 3D breast cancer models. Additionally, a recent study by DeCarlo et al.[5] documented that a folic acid-conjugated poly(styrene-alt-maleic anhydride) (SMA) copolymer resulted in dual therapeutic anticancer potential to treat cancer, as it was evident on breast and prostate cancer cell lines. Anticancer agents from natural sources are widely explored so as to avoid the downsides of synthetic drugs. Sometimes these synthetic drugs were not effective alone and had side effects. Researchers combined chemotherapy with alternative therapies like targeted chemotherapy and immunotherapy to develop immune conjugates, which can overcome their drawbacks.[1] To date, the drug resistance and controlled delivery of these

Received: November 10, 2021
Accepted: January 26, 2022
Published: February 3, 2022

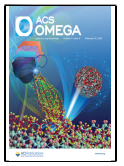

conjugates to the cancer site are still major concerns that need to be explored.

Researchers have developed various inorganic and organic nanocarriers and exploited them for delivering therapeutic agents to cancer sites. Metallic nanoparticles, quantum dots, carbon nanotubes, liposomes, micelles, dendrimers, polymeric nanoparticles, and silica nanoparticles have revolutionary applications in the biomedical field.[6,7] Some of them are already in the preclinical and clinical stages.[8] Polymeric nanoparticles are an effective nanocarrier because of their excellent properties such as biocompatibility, biodegradability, nontoxicity, nonimmunogenicity, and controlled drug delivery.[6] The polylactic acid−poly(ethylene glycol) (PLA−PEG) multiblock copolymer is of major interest regarding consideration as a drug carrier. PLA segments provide rigidity to the carrier, whereas the PEG part confers stealth behavior.[9] Due to the stealth property, nanoparticles can escape from the immune system. Moreover, they can be circulated for a longer time after injection, which increases their life span. PEG also provides hydrophilicity to certain chemotherapeutic hydrophobic drugs, thus increasing their solubility.[10,11] Researchers have encapsulated and conjugated various anticancer agents such as chemo drugs, aptamers, nucleic acids, and peptides with nanoparticles of the PLA−PEG copolymer.[12−17]

Moreover, biosurfactants have recently emerged as promising molecules having great applications in the biomedical field.[18,19] These biomolecules isolated from microbial sources are lipopeptides, glycolipids, and glycoproteins in nature. They have shown anticancer properties mostly via inducing the apoptosis pathway.[18] In our previous studies, a biosurfactant isolated from *Candida parapsilosis* has been reported to have anticancer properties. The novel biosurfactant was conjugated with graphene quantum dots to obtain a theranostic tool. It showed cytotoxic effects against the MCF-7 cell line.[20] However, for controlled and sustained release of the drug, polymeric nanoparticles are preferred as a delivery agent.[14,15,17,21,22] Moreover, polymeric nanoparticles protect the encapsulated drug from degradation by the immune system because of their stealth behavior.

In our present study, we propose the controlled delivery of biosurfactant via PLA−PEG copolymeric nanoparticles. For targeted delivery, folic acid is used as a ligand that targets the folic acid receptors overexpressed on cancer cells. We study the cytotoxicity of the nanoformulations against the MDA-MB-231 breast cancer cell line. The biosurfactant kills cancer cells by apoptosis induction. The release kinetics from polymeric nanoparticles is also determined in vitro. Based on this work, a biosurfactant isolated from *C. parapsilosis* loaded in polymeric nanoparticles can be explored as a promising therapeutic system.

2. MATERIALS AND METHODS

2.1. Chemicals and Materials. PLA (72 kDa) and PEG (4 kDa) were purchased from NatureWorks and Fisher Scientific, respectively. Kolliphor TPGS was purchased from BASF. Hydrochloric acid was purchased from Rankem. Organic solvents such as acetonitrile were obtained from Merck, dichloromethane (DCM) and diethyl ether were purchased from Rankem, and methanol was purchased from Fisher Scientific. Rhodamine B and DAPI were purchased from Sigma-Aldrich. Folic acid and 4-dimethylaminopyridine (DMAP) were purchased from SRL. *N*,*N*-Dicyclohexylcarbodiimide (DCC) was purchased from Tokyo Chemical Industry Co., Ltd., (TCI). Potato dextrose broth medium, dialysis bag, phosphate-buffered saline (PBS), trypsin, MTT reagent, and DMSO were purchased from HiMedia. RPMI-1640 was purchased from Lonza. FBS, penicillin, and streptomycin were purchased from Gibco. The human breast cancer cell line MDA-MB-231 was a gift from Dr. Ashok Kumar Yadav (Department of Experimental Medicine and Biotechnology, PGIMER, Chandigarh).

2.2. Biosurfactant Synthesis. The biosurfactant was synthesized from *C. parapsilosis* isolated previously in the laboratory. The culture was grown in potato dextrose broth for 72 h under anaerobic conditions at 37 °C. After the incubation period, microbial cells were separated from the broth by centrifuging at 6000 rpm for 20 min. The supernatant was collected in a beaker and the pH was set at 2.0 by adding a 0.1 N hydrochloric acid solution. It was kept overnight at 2−4 °C to precipitate the synthesized biosurfactant. The next day, it was centrifuged at 12 000 rpm at 2 °C for 20 min to separate the precipitated biosurfactant from the broth. The pellet was collected and lyophilized. This freeze-dried biosurfactant was used for further studies. Culture conditions and extraction of the biosurfactant were according to the previous standardized protocol of the laboratory.[23]

2.3. Synthesis and Characterization of the PLA−PEG Copolymer. The PLA−PEG copolymer was synthesized using PLA (72 kDa) and PEG (6 kDa) as reported by Kumar et al.[17] Equal amounts (0.014 mmol) of PLA and PEG were dissolved in 100 mL of DCM with continuous stirring at 0−2 °C. To the solution, 5 mL of 1% DCC was added slowly. After that, 2 mL of 0.1% DMAP was added dropwise to the solution. DCC and DMAP were used as catalysts to covalently link PLA and PEG, respectively. The mixture was stirred for 16 h with a magnetic stirrer. The unreacted polymer was removed using a 1:1 mixture of diethyl ether and methanol. The resulting copolymer was precipitated and lyophilized. Proton nuclear magnetic resonance spectrometry (^{1}H NMR, Bruker Avance II 400 NMR spectrometer) of the PLA−PEG copolymer was performed in $CDCl_3$ to confirm its synthesis.[17]

2.4. Conjugation of the Polymer with Folic Acid (FA). FA was coupled with the PLA−PEG copolymer for the targeted delivery of copolymer nanoparticles. DCC and DMAP were used as catalysts for the conjugation. One equivalent of the PLA−PEG copolymer and 2.5 equiv of DCC were dissolved in DMSO containing 2.5 equiv of folic acid and 0.5 equiv of DMAP. This reaction mixture was stirred in an argon atmosphere for 6 h at room temperature. The mixture was filtered to remove the byproduct, DCU. Unreacted folic acid was removed from the filtrate by dialysis for 48 h against distilled water. The distilled water was regularly changed. The resulting product was lyophilized to obtain the FA-conjugated PLA−PEG copolymer.[24] The conjugation of folic acid was confirmed by analyzing the peaks of ^{1}H NMR.

2.5. Nanoparticle Synthesis. The nanoparticles of the biosurfactant-loaded PLA−PEG copolymer, biosurfactant-loaded FA-conjugated PLA−PEG copolymer, Rhodamine B-loaded PLA−PEG copolymer, and Rhodamine B-loaded FA-conjugated copolymer as well as void nanoparticles were synthesized by the double emulsion solvent evaporation method.[17,25] The organic phase was prepared by dissolving the PLA−PEG copolymer (6 mg) and the biosurfactant (2 mg) in 1 mL of acetonitrile (3:1 ratio). To prepare fluorescent dye-labeled nanoparticles, 100 μL of Rhodamine B dye from a 1 mg/mL stock solution was dissolved in acetonitrile solution

https://doi.org/10.1021/acsomega.1c06338
ACS Omega 2022, 7, 5231−5241

containing 10 mg of the polymer. The organic phase was emulsified dropwise with 10 mL of an aqueous solution containing 0.3% TPGS by vortexing vigorously. After that, ultrasonication of the emulsion was done for 2 min to facilitate nanoparticles. Void nanoparticles were synthesized with the same process except biosurfactant and the dye was not added. Then, the emulsion was stirred with a magnetic stirrer at room temperature for 6−8 h to evaporate the solvent and stabilize the nanoparticles. The nanoparticles were collected and washed three times with distilled water by centrifuging at 10 000 rpm for 10 min. They were freeze-dried and stored at −20 °C until use. The supernatant was collected and analyzed for free biosurfactant using a UV−visible spectrophotometer. The nanoparticles were further characterized to confirm their synthesis and determine their size and morphology. Each experiment was carried out in triplicate.

2.6. Characterization of Nanoparticles. The particle size, polydispersity index (PDI), and charge were determined using a Zetasizer (Beckman Coulter, Delsa) in triplicate. The morphology of the nanoparticles was determined by microscopy techniques such as field emission scanning electron microscopy (SU 8010 series, Hitachi, Japan) and transmission electron microscopy (H-7500, Hitachi, Japan).

2.7. Encapsulation Efficiency. Encapsulation efficiency is the percentage of drug that is successfully loaded into the nanoparticles. Loading capacity is the amount of drug loaded per unit weight of the nanoparticle. The amount of biosurfactant encapsulated in the polymeric nanoparticles was calculated using a UV−visible spectrophotometer. The synthesized nanoparticles were centrifuged at 10 000 rpm for 10 min, and the supernatant was stored. The free biosurfactant that remained in the supernatant was determined by measuring the absorbance at 265 nm. The amount of the free biosurfactant was calculated from the standard curve prepared by measuring the absorbance of standard solutions of the biosurfactant in the UV−visible spectrophotometer. The analysis was done in triplicate, and the results are presented as mean. The formulae for encapsulation efficiency (EE%) and drug loading capacity (DL%) are mentioned below.[17]

$$\text{EE\%} = \frac{\text{biosurfactant (total)} - \text{free biosurfactant}}{\text{biosurfactant (total)}} \times 100$$

$$\text{DL\%} = \frac{\text{biosurfactant (total)} - \text{free biosurfactant}}{\text{polymer(total)}} \times 100$$

2.8. Assessment of Biosurfactant Release from Nanoparticles. The in vitro release profile of the biosurfactant was determined in phosphate-buffered saline (PBS, pH 7.2) by the dialysis bag method at different time points. This technique is widely used in in vitro drug release studies. It is based on the diffusion of small solutes from a concentrated solution to a lower-concentration solution of this solute through a semipermeable membrane until equilibrium is reached. PBS provides the simulated conditions of our body. Briefly, 1 mL of the nanoparticle suspension in PBS consisting of 2 mg of the biosurfactant entrapped in 6 mg of the polymer was immersed in the dialysis bag (cutoff molecular weight: 10 000 Da). This dialysis bag was submerged completely into 19 mL of PBS solution. The solution was continuously stirred at room temperature with a magnetic stirrer. Then, 2 mL of the released medium was taken out at designated time points (0.25, 0.5, 2, 4, 6, 8, 12, 24, 48, 72, 96, 120 h) and an equal volume of fresh PBS was added to the reaction mixture. The amount of the released biosurfactant was determined using a UV−visible spectrophotometer at 265 nm from the standard curve of the biosurfactant. To study the release kinetics, data obtained from in vitro drug release studies were plotted as the cumulative amount of drug release versus time. The cumulative drug release percentage was calculated by adding the amount of drug released at each time point.[26,27] The experiment was performed in triplicate and drug release was calculated as mean.

2.9. Kinetic Analysis of Dissolution Data. The data obtained from in vitro release studies were analyzed to find the mechanism of biosurfactant release. The obtained data were fitted to various models like zero-order model, first-order model, Higuchi model, and Hixson−Crowell erosion equation. The best fit for each model was determined by analyzing their correlation coefficient (R^2).[27,28] To find the dissolution mechanism of drug release from the matrix, the data were further plotted in the Korsmeyer−Peppas model. The release exponent (n) is obtained from the slope of the plot of the log cumulative % of drug released versus log time. Its value is used to characterize different release mechanisms.[27−29]

2.10. In Vitro Anticancer Activity. The polymeric nanoparticles were evaluated for in vitro cytotoxicity against cancer cells using the 3-(4, 5-dimethylthiazol-2-yl)-2,5-diphenyltetrazolium bromide (MTT) assay on the MDA-MB-231 cell line (breast cancer). The cells were grown in an RPMI-1640 medium containing 10% FBS, 100 U·mL^{-1} penicillin and streptomycin at 37 °C, and 5% CO_2 for 2−3 days. The prepared nanoparticles were diluted with RPMI medium to obtain final concentrations of 3.75, 7.5, 15, 30, and 60 μg/mL of nanoparticles. The cells were grown on a 96-well plate at a density of 5 × 10^3 cells/well. After overnight incubation, nanoparticles solutions were added to respective wells and incubated for 24, 48, 72, and 96 h in 5% CO_2 at 37 °C. Afterward, 100 μL of the MTT solution (0.5 mg/mL in PBS) was added to each well and incubated for 4 h followed by DMSO addition. The absorbance of produced formazan was monitored on an ELISA reader at 560 nm. Void nanoparticles were taken as control, and the results were compared with different biosurfactant-loaded nanoparticle groups and the free biosurfactant. The percentage cell viability was calculated using the following formula. The experiments were performed in triplicate, and the results are presented as mean.

$$\text{cell viability (\%)} = \frac{\text{mean optical density of test}}{\text{mean optical density of control}} \times 100$$

2.11. Cellular Uptake. The cellular uptake of nanoparticles in cancer cells was assessed by confocal laser scanning microscopy (CLSM). MDA-MB-231 cells were incubated with Rhodamine B-loaded nanoparticles (PLA−PEG copolymer and FA PLA−PEG copolymer) in six-well plates. After 3, 6, and 12 h, nuclei of the cells were stained with DAPI and the cells were washed with PBS twice to remove free DAPI. The cells were visualized under a confocal laser scanning microscope (CLSM) with appropriate filters.

2.12. Apoptosis Assay. The apoptosis assay of the treated cancer cell line was done to determine the killing mechanism of our synthesized nanoparticles. Annexin V-Alexa Fluor 488/PI Apoptosis Assay Kit (Invitrogen) was used for the analysis. The results were analyzed by confocal laser scanning microscopy (CLSM) and compared among free biosurfactant,

https://doi.org/10.1021/acsomega.1c06338
ACS Omega 2022, 7, 5231−5241

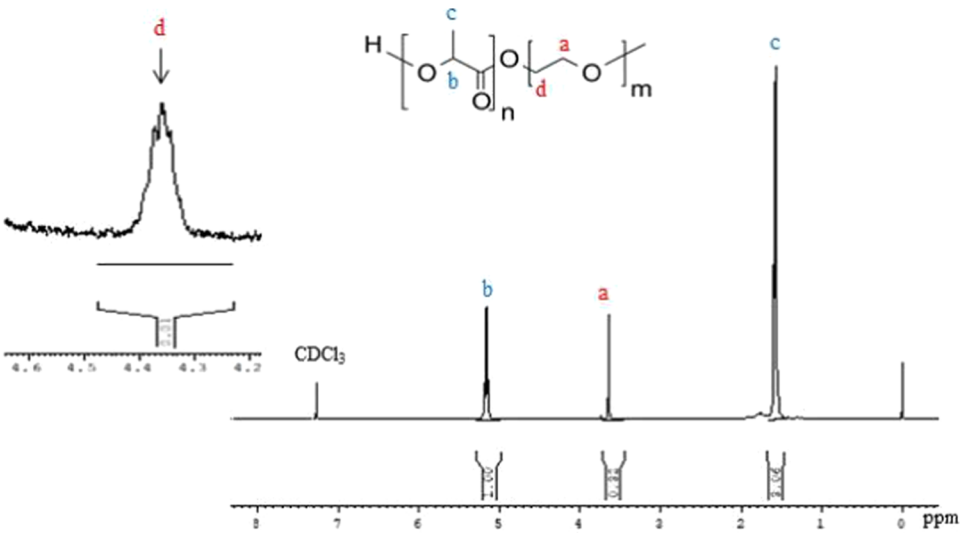

Figure 1. ^{1}H NMR spectrum of the synthesized PLA−PEG copolymer in $CDCl_3$ as a solvent.

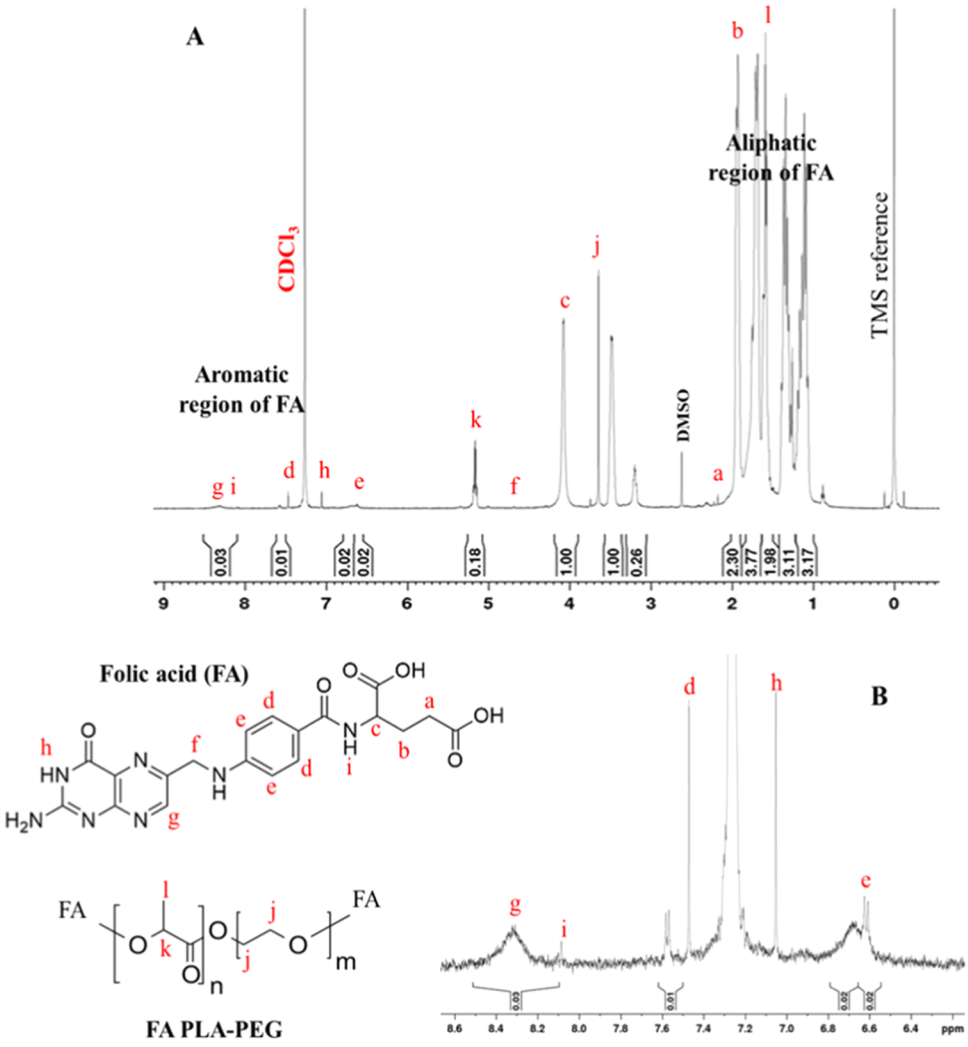

Figure 2. (A) ^{1}H NMR spectrum of the folic acid-conjugated PLA−PEG copolymer in $CDCl_3$ as a solvent. (B) Aromatic region of the ^{1}H NMR spectrum of the folic acid-conjugated PLA−PEG copolymer.

biosurfactant-loaded PLA−PEG nanoparticles, and biosurfactant-loaded FA PLA−PEG nanoparticles. The cells were treated with nanoparticles for 24 h. The concentration of the biosurfactant was set at 20 μg/mL. After the treatment period, the cells were stained with Annexin V-Alexa Fluor 488 and propidium iodide solution for 5 min at room temperature in

https://doi.org/10.1021/acsomega.1c06338
ACS Omega 2022, 7, 5231−5241

1× Annexin binding buffer. After that, the cells were washed, fixed in a 2% formaldehyde solution, and analyzed under CLSM.[17]

2.13. Statistical Analysis. The values of all of the results were expressed as mean with standard deviation (mean ± SD). The statistical level of significance was set at $P < 0.05$ for all comparisons. Data were analyzed using two-way ANOVA without replication.

3. RESULTS AND DISCUSSION

3.1. Synthesis and Characterization of the Copolymer. PLA and PEG polymers were successfully conjugated together with the help of DCC and DMAP to synthesize the PLA−PEG block copolymer. DCC helps in coupling the carboxyl group of PLA and the dihydroxyl group of PEG, and DMAP acts as a catalyst. The ζ-potential of the PLA−PEG−FA conjugate was found to be −15.47 mV and that of biosurfactant-encapsulated PLA−PEG-FA was found to be −12.51 mV. The coupling of PLA and PEG was confirmed by analyzing the peaks of ^{1}H NMR of the synthesized copolymer (Figure 1). The spectra showed peaks at 5.2 and 1.6 ppm, which represent the protons of methine (−CH) and methyl ($-CH_3$) groups of lactic acid repetitive units, respectively. The peak at 3.64 ppm represents protons of the methylene group (CH_2-) in the PEG blocks. The formation of the copolymer was verified by the presence of peaks at 4.3 ppm, which is associated with protons of the methylene group at the end of PEG chains attached to the methylene groups of lactide monomers.[17,22] These results confirmed that polymers were coupled successfully.

3.2. Conjugation of Folic Acid with the PLA−PEG Copolymer. The PLA−PEG copolymer was conjugated with folic acid to specifically target the cancer cells and increase the internalization of nanoparticles to the targeted site. ^{1}H NMR spectra of this conjugate have confirmed that folic acid was conjugated successfully (Figure 2A). Peaks at 5.2 and 1.6 ppm (corresponding to PLA) and 3.64 ppm (corresponding to the PEG proton) confirmed the presence of the copolymer. The small peaks at 6.6 ppm (e) and 7.5 ppm (d) are attributed to aromatic protons of folic acid, and the peak at 8.3 ppm (g) is attributed to the pteridine proton of folic acid. The peaks of other protons of folic acid are also mentioned in Figure 2B.[12,13,30] These peaks have confirmed the conjugation of folic acid with the copolymer.

3.3. Synthesis and Characterization of PLA−PEG Nanoparticles. Nanoparticles were prepared by the double emulsion solvent evaporation method. The nanoparticles synthesized gave a clear bluish appearance without any aggregation, which depicts that nanoparticles were formed. Folic acid-conjugated nanoparticles appeared yellow due to the yellow color of folic acid. Biosurfactant-loaded nanoparticles were denser. The structure of these nanoparticles is a bilayer as reported by Kumar et al. PLA formed the hydrophobic core, and the outer hydrophilic layer was given by PEG.[17] The average hydrodynamic diameter of PLA−PEG nanoparticles, determined by the dynamic light scattering method (Beckman Coulter, Delsa), was 223.4 nm. The polydispersity index of these nanoparticles was 0.177, which is within the acceptable range for polymeric nanoparticles.[31] The size distribution of these nanoparticles is given in Figure 3.

Transmission electron microscopy (TEM) and field emission scanning electron microscopy (FE-SEM) studies have shown that the nanoparticles are spherical in shape and uniform with average diameters of the void and biosurfactant-loaded nanoparticles of 30 and 60 nm, respectively (Figure 4). It can be analyzed from TEM images (Figure 4A,B) that after loading the biosurfactant, the size of nanoparticles has increased.

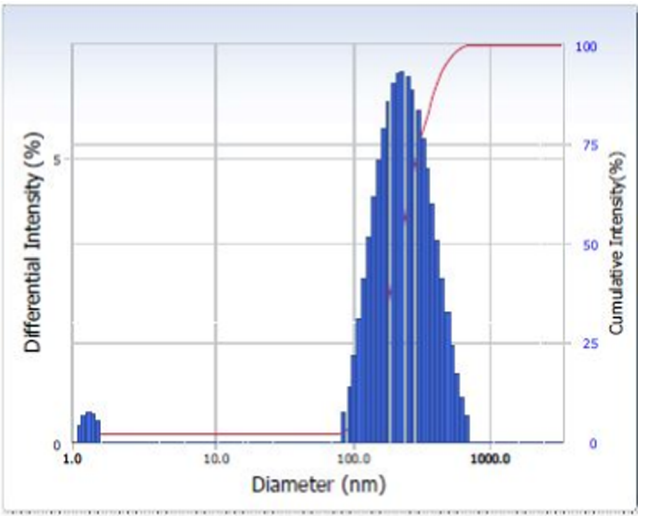

Figure 3. Size distribution of PLA−PEG nanoparticles.

3.4. Encapsulation Efficiency. The amount of biosurfactant encapsulated in polymeric nanoparticles determines the effectiveness of synthesized nanoformulations. The encapsulation efficiency of these nanoparticles was determined by measuring the free amount of biosurfactant in the nanoformulation. The standard plot of biosurfactant in phosphate-buffered saline (PBS) was plotted at 265 nm. The encapsulation efficiency of these nanoparticles was calculated as 84.9%. The drug loading % was found to be 28.3%. These results displayed good encapsulation efficiency; hence, the prepared biosurfactant-loaded nanoparticles are expected to have superior cytotoxicity activity.

3.5. In Vitro Biosurfactant Release Study. The in vitro release of the biosurfactant from polymeric nanoparticles was assessed under simulated body conditions at 7.2 pH for up to 120 h. Figure 5 shows the cumulative release of biosurfactant (%) versus time curve of the biosurfactant from biosurfactant-loaded PLA−PEG nanoparticles in vitro during 5 days. The study has exhibited that the release of the pure biosurfactant was found to be 100% by 30 h and 88% for nanoformulations after 3 days. Thereafter, it was observed that the release was slowed down and 98% of the biosurfactant was released in 5 days.

3.6. Kinetic Analysis. The in vitro release profile data were plotted and fitted in different mathematical models. The release rate kinetics data of the PLA−PEG nanoparticles are shown in Table 1. Based on the values of correlation coefficients from kinetic data, it is concluded that the biosurfactant-loaded polymeric nanoparticles showed a good correlation to the Higuchi model. This model describes the study of the release of water-soluble and less-soluble drugs encapsulated in semisolid and/or solid matrixes.[32] According to this model, the release of drugs from the insoluble matrix is dependent on the square root of time and is based on Fickian diffusion. It can be interpreted that the prime mechanism of biosurfactant release is the diffusion-controlled release mechanism.[28,29] Once the prime mechanism of drug release

https://doi.org/10.1021/acsomega.1c06338
ACS Omega 2022, 7, 5231−5241

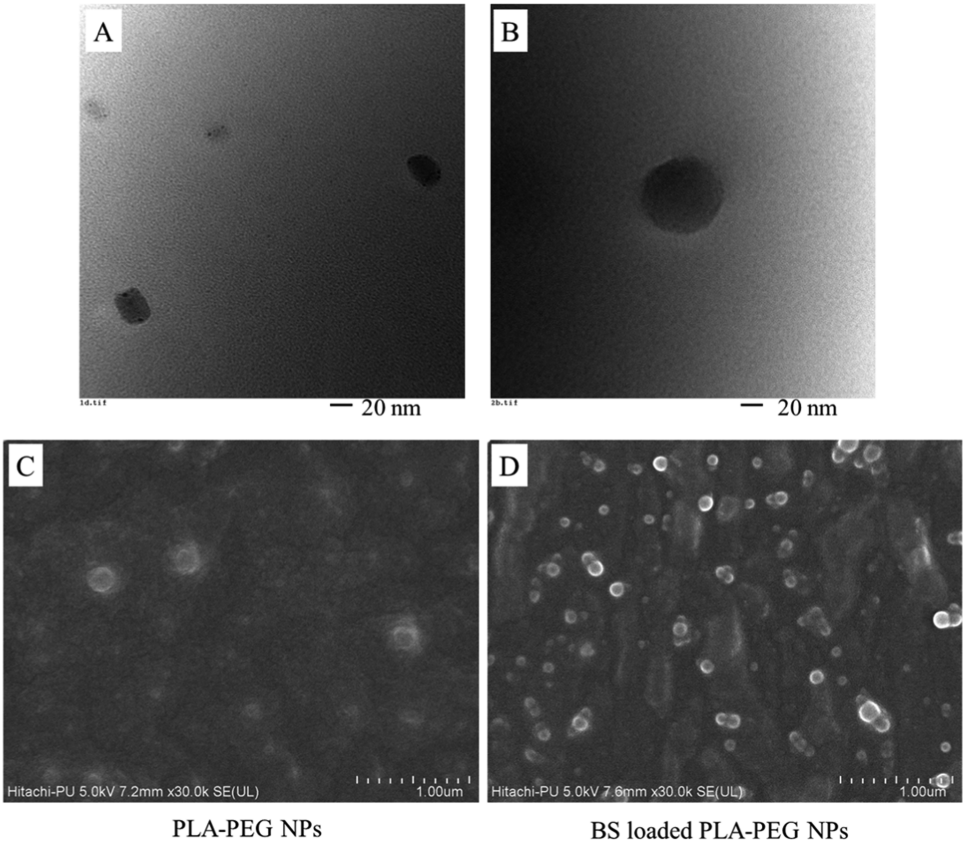

Figure 4. (A, B) TEM images of plain and BS-loaded PLA−PEG nanoparticles. (C, D) FE-SEM images of plain and BS-loaded nanoparticles (NPs—nanoparticles and BS—biosurfactant).

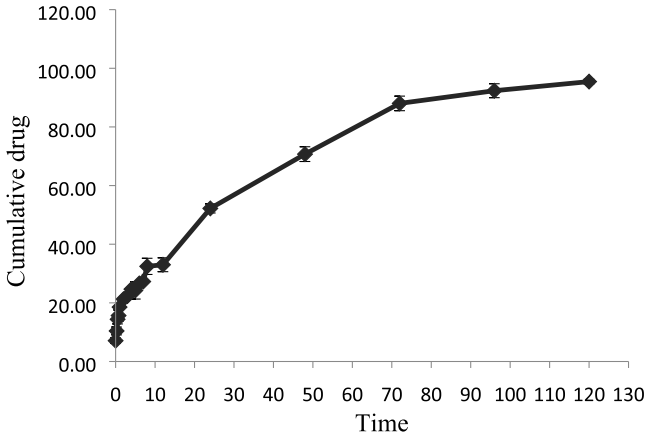

Figure 5. In vitro release profile of biosurfactant from PLA−PEG nanoparticles.

was confirmed to be diffusion-controlled from the Higuchi plot, then the type of diffusion needed to be determined. The Korsmeyer−Peppas model was used to analyze the mechanism of drug release. The graph was plotted as log cumulative drug release % versus log time. The release exponent (n) was obtained from the graph by determining its slope. The value of n was below 0.45, which indicates that the drug release was controlled by Fickian diffusion.[32−34]

3.7. Cellular Uptake Study. Nanoparticles loaded with Rhodamine B were used to assess the uptake of nanoparticles in MDA-MB-231 cancer cells. These nanoparticles were internalized in the cells within 3−6 h. The CLSM images are shown in Figure 6a,b. The nuclei of the cells were stained with DAPI, as shown in Figure 6a, which shows the CLSM images of the control. The internalization of nanoparticles was higher at 6 h (Figure 6b). The cellular uptake of folic acid-conjugated nanoparticles was higher compared to plain nanoparticles because of the active cell targeting of these nanoparticles.

3.8. In Vitro Cytotoxicity Assay. In our recent study, the toxicity of the biosurfactant and its nanoparticles was evaluated in a normal healthy mouse and no significant toxicity was observed for this biosurfactant-loaded nanoformulation.[35] In the present study, the effect of biosurfactant-loaded nanoparticles was studied on the growth of the MDA-MB-231 breast cancer cell line. The study was done for 4 days at different concentrations of nanoparticles (3.75, 7.5, 15, 30, 60 μg/mL). The results of both FA-conjugated and plain polymeric nanoparticles were compared. As the polymer-to-biosurfactant ratio is 3:1, the concentration of the biosurfactant was taken as 1.25, 2.5, 5, 10, and 20 μg/mL for encapsulating

Table 1. Correlation Coefficient (R^2) and Release Exponent (n) of the Kinetic Data Analysis of Biosurfactant Release from PLA−PEG Nanoparticles

mathematical models	zero-order model	first-order model	Higuchi model	Hixson−Crowell model	Korsmeyer−Peppas model	
correlation coefficient (R^2)	0.9222	0.7138	0.9893	0.8079	0.9099	n = 0.3879

https://doi.org/10.1021/acsomega.1c06338
ACS Omega 2022, 7, 5231−5241

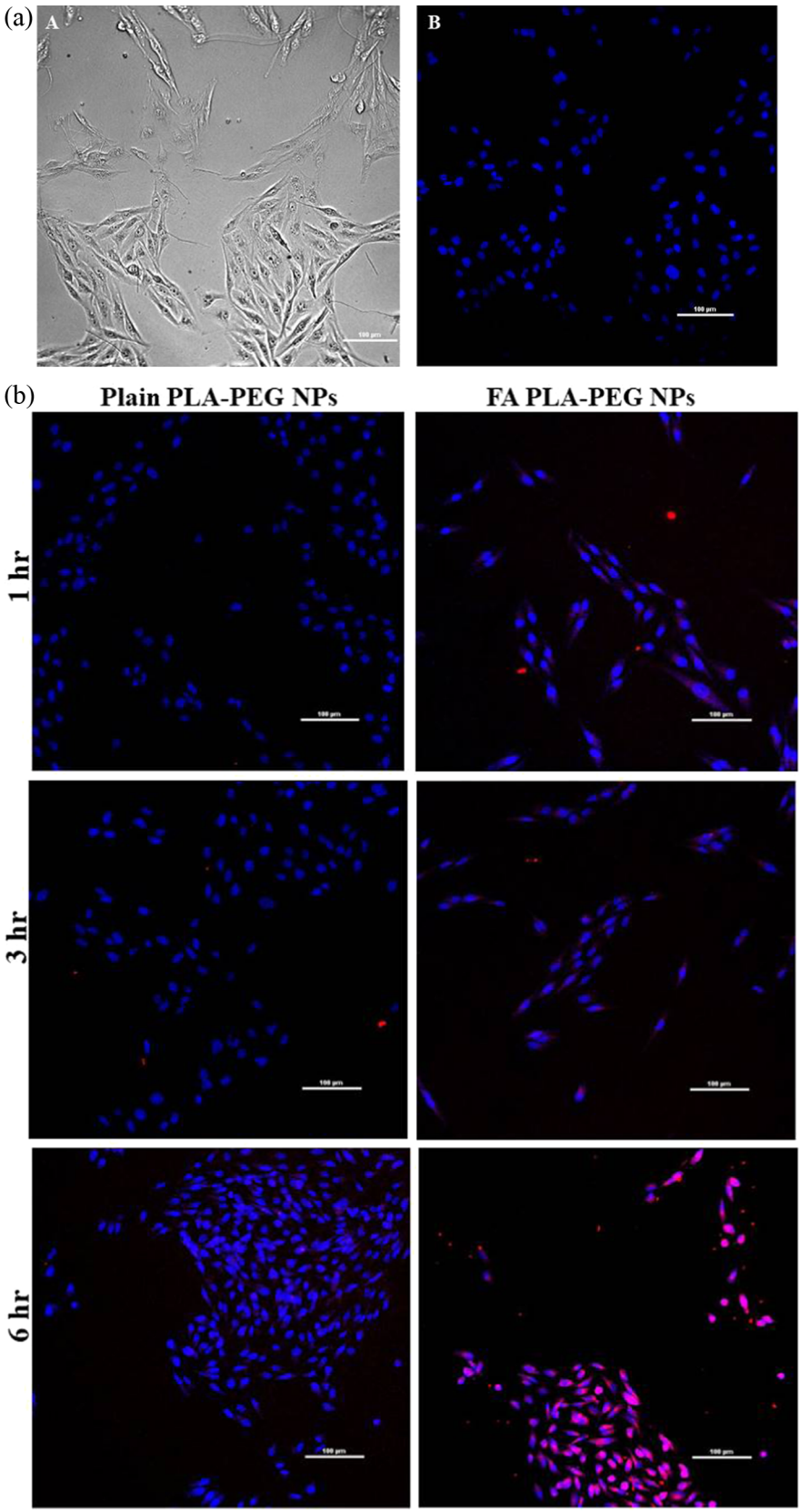

Figure 6. (a) CLSM images of MDA-MB-231 cancer cells under bright field (A) and dark field of nuclei stained with DAPI excited by a 405 nm laser (B). Scale bar: 100 μm. (b) Cellular uptake of Rhodamine B-loaded plain and folic acid-conjugated PLA−PEG nanoparticles. Scale bar: 100 μm (NPs—nanoparticles and FA—folic acid).

in the PLA−PEG copolymer with concentrations of 3.75, 7.5, 15, 30, and 60 μg/mL, respectively. In our previous study done by Bansal et al., the cytotoxicity of the biosurfactant was observed for two concentrations (2.5 and 5 μg/mL) in the

https://doi.org/10.1021/acsomega.1c06338
ACS Omega 2022, 7, 5231−5241

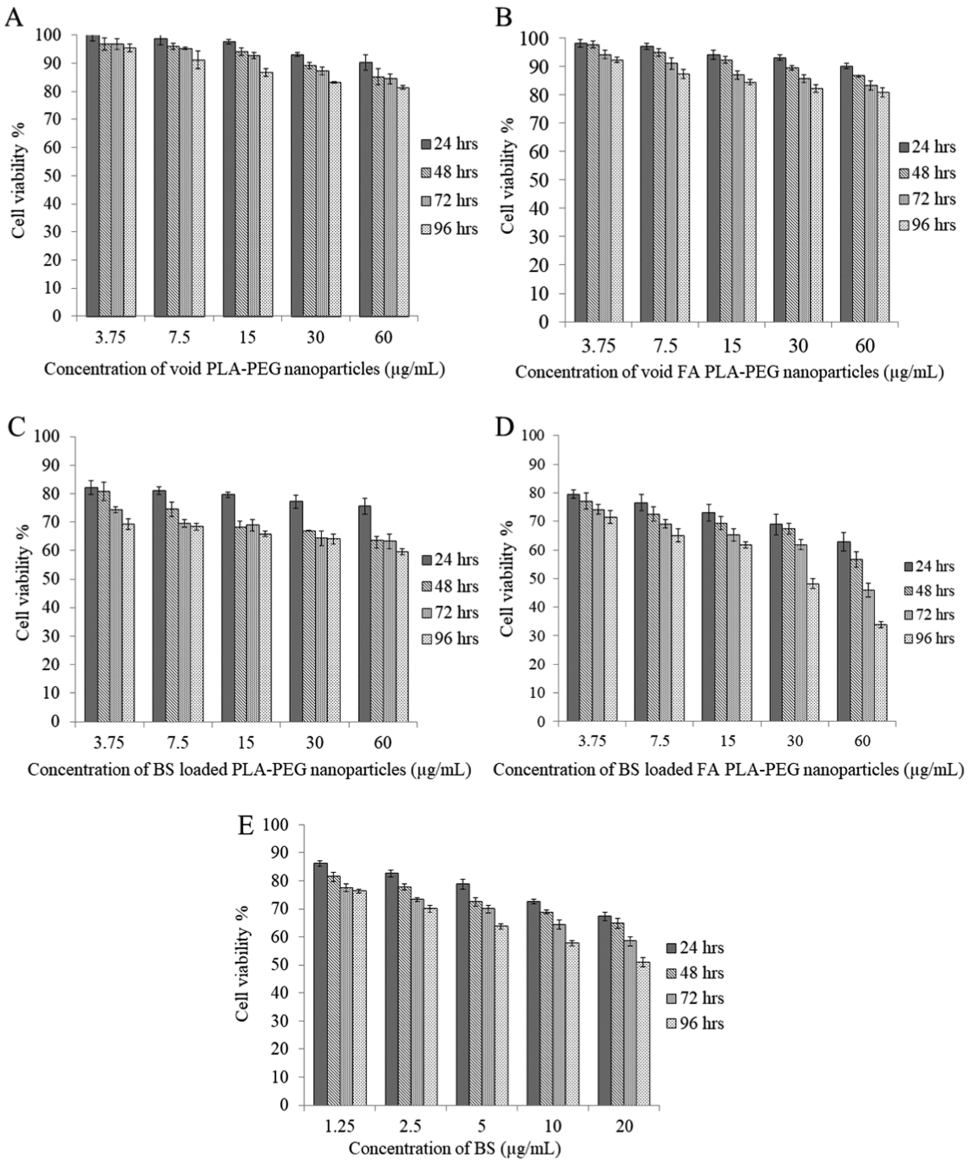

Figure 7. MTT cytotoxicity assay: (A, B) cytotoxicity of void and FA-conjugated polymeric nanoparticles (concentrations: 3.75, 7.5, 15, 30, 60 μg/mL); (C, D) cytotoxicity of BS (concentrations: 2.5 and 5 μg/mL)-loaded and FA-conjugated polymeric nanoparticles (ratio 3:1); and (E) cytotoxicity of free BS against the MD-MB-231 breast cancer cell line at different time points (BS—biosurfactant).

MCF-7 breast cancer cell line. Based on this study, concentrations lower and higher than these concentrations were selected for the present study to effectively analyze the effect of the biosurfactant on a different breast cancer cell line (MDA-MB-231). It was observed that empty nanoparticles without biosurfactant had little effect on the viability of cancer cells. At a higher concentration (60 μg/mL), the cell viability for void plain and FA PLA−PEG nanoparticles on the 4th day was ∼80% (Figure 7A,B). Hence, it can be claimed that polymeric nanoparticles are not much toxic against cancer cells. Cells treated with biosurfactant alone showed 51% cell viability after 96 h at the highest concentration (Figure 7E). Biosurfactant-loaded plain PLA−PEG nanoparticles showed 60% cell viability at the highest concentration after 96 h (Figure 7C). Moreover, when the polymer was conjugated with folic acid, cell viability reduced to 33% (Figure 7D). Hence, folic acid-conjugated nanoparticles actively targeted the cancer cells and delivered a therapeutic agent to the target site more efficiently. In normal human cells, the expression of these receptors is significantly low.[36] All of the data were statistically analyzed by two-way ANOVA with the significance level set at 5%. The F value was found to be greater than the critical F value, which determined that the differences between the cell viability of the cell line at different time points and different concentrations were significant.

3.9. Apoptosis Assay. To determine the killing mechanism of biosurfactant-loaded nanoparticles, the apoptosis assay was done. MDA-MB-231 cells were treated with free biosurfactant and biosurfactant-loaded PLA−PEG and FA PLA−PEG nanoparticles. These treated cells were further monitored for externalization of phosphatidylserine (PS) at the cell membrane. Apoptotic cells translocate PS from the inner to outer leaflet of the plasma membrane. Annexin V labeled with a fluorophore is a human anticoagulant that binds to the exposed PS on the cells. Propidium iodide is a red fluorescent dye that binds to the nucleic acids of dead cells. Apoptotic cells give green fluorescence, and necrotic cells give red fluorescence. Confocal images of the cells demonstrated that

https://doi.org/10.1021/acsomega.1c06338
ACS Omega 2022, 7, 5231−5241

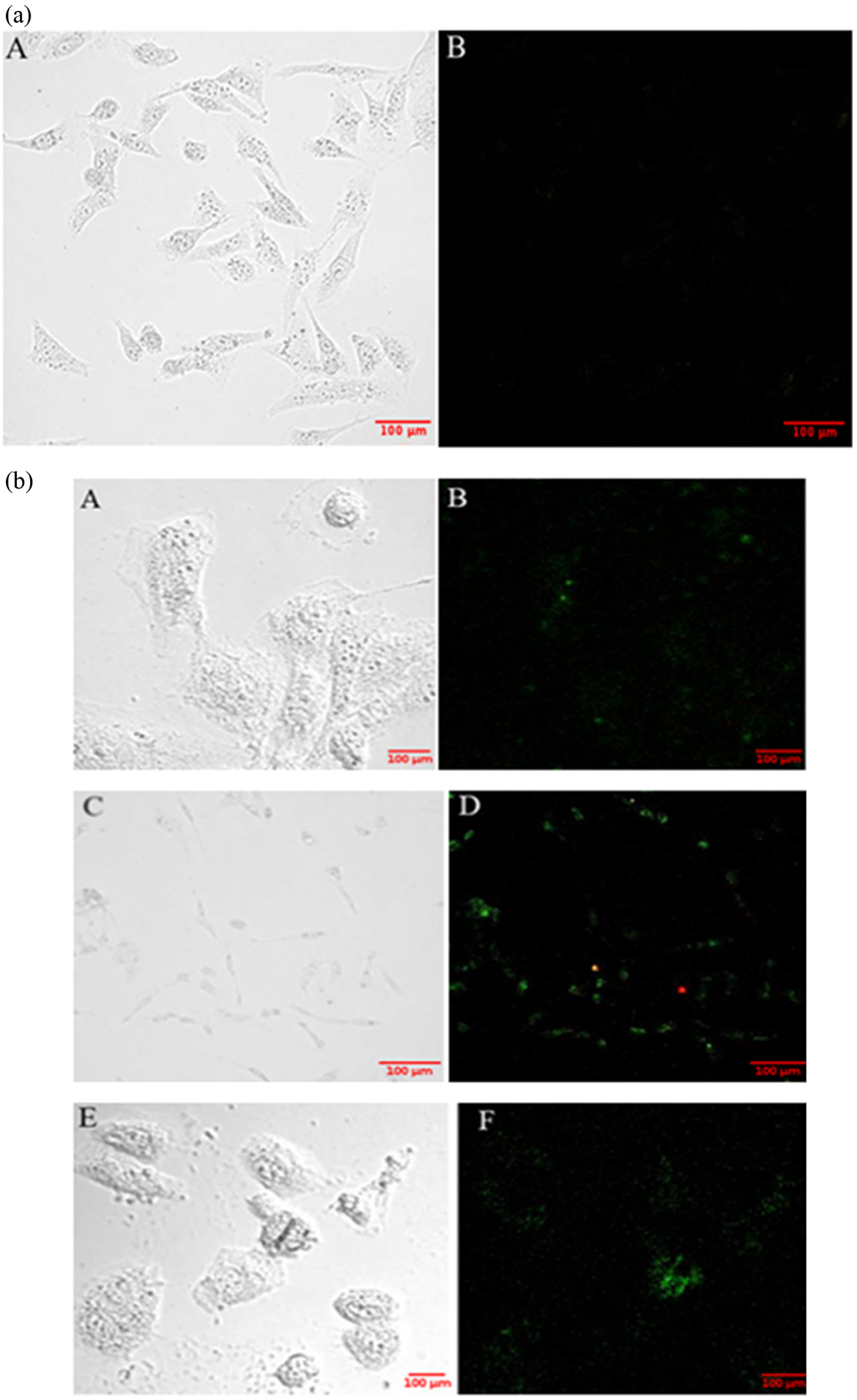

Figure 8. (a) Confocal microscopy images of control cells: (A) bright-field and (B) confocal images with appropriate filters. Scale bar: 100 μm. (b) Confocal microscopy images of cells treated with free biosurfactant: (A, B) biosurfactant-loaded PLA−PEG nanoparticles; (C, D) biosurfactant-loaded FA PLA−PEG nanoparticles; and (E, F) green fluorescence indicates that the biosurfactant induces apoptosis in MDA-MB-231 cells (breast cancer). Scale bar: 100 μm.

https://doi.org/10.1021/acsomega.1c06338
ACS Omega 2022, 7, 5231−5241

the cells treated with free biosurfactant and biosurfactant-loaded nanoparticles (both plain and FA-conjugated) underwent apoptosis (Figure 8a,b). Figure 8a shows the confocal image of control cells. No fluorescence was observed in untreated cells. Thus, biosurfactant induced apoptosis in cancer cells.

4. CONCLUSIONS

The present study emphasized on a novel therapeutic tool to control cancer by encapsulating a biosurfactant in PLA−PEG copolymeric nanoparticles. The encapsulation efficiency of this system was 84.9%. The release profile of the biosurfactant from these nanoparticles showed the sustained release of the biosurfactant in saline buffer. Approximately 98% of the biosurfactant was released from this formulation in 120 h. It was observed from kinetic models that the biosurfactant was released by Fickian diffusion from the polymeric matrix. Further, the folate ligand was conjugated with the PLA−PEG copolymer to obtain active targeting of the system in cancer cells. This formulation showed maximum internalization and superior cytotoxicity compared to nontargeting ones against the breast cancer cell line (MDA-MB-231). Moreover, it was observed that this formulation induced apoptosis in the breast cancer cell line and thereby killed cancer cells. Therefore, PLA−PEG polymeric nanoparticles can be exploited as a suitable vehicle for the controlled release of a novel biosurfactant isolated from *C. parapsilosis*, to control breast cancer cells.

AUTHOR INFORMATION

Corresponding Authors

Gurpal Singh − *University Institute of Pharmaceutical Sciences, Panjab University, Chandigarh 160014, India*; Email: gurpalsingh.ips@gmail.com

Mary Chatterjee − *Biotechnology Branch, University Institute of Engineering and Technology, Panjab University, Chandigarh 160014, India*; orcid.org/0000-0001-8118-8495; Email: maryc@pu.ac.in

Authors

Aishani Wadhawan − *Biotechnology Branch, University Institute of Engineering and Technology, Panjab University, Chandigarh 160014, India*

Joga Singh − *University Institute of Pharmaceutical Sciences, Panjab University, Chandigarh 160014, India*

Himani Sharma − *Department of Zoology, Panjab University, Chandigarh 160014, India*

Shristi Handa − *Biotechnology Branch, University Institute of Engineering and Technology, Panjab University, Chandigarh 160014, India*

Ravinder Kumar − *Department of Zoology, Panjab University, Chandigarh 160014, India*

Ravi Pratap Barnwal − *Department of Biophysics, Panjab University, Chandigarh 160014, India*; orcid.org/0000-0003-3156-5357

Indu Pal Kaur − *University Institute of Pharmaceutical Sciences, Panjab University, Chandigarh 160014, India*

Complete contact information is available at: https://pubs.acs.org/10.1021/acsomega.1c06338

Author Contributions

M.C., G.S., and I.P.K.: conceptualization. A.W., J.S., G.S., and M.C.: work design. A.W., H.S., and J.S.: data acquisition and analysis. A.W., R.K., R.P.B., G.S., and M.C.: data interpretation. R.K., I.P.K., G.S., M.C., and R.P.B.: resources. A.W.: writing original draft. A.W. and M.C.: review and editing draft. M.C., G.S., and I.P.K.: supervision. All authors read and approved the final manuscript.

Funding

This work was supported by University Grants Commission (UGC), Basic Scientific Research, Government of India (Sanction No. F.30-301/2016 [BSR], dated 16.02.2017).

Notes

The authors declare no competing financial interest.

ACKNOWLEDGMENTS

The authors gratefully acknowledge the support of Dr. Ashok Kumar Yadav, Assistant Professor, Department of Experimental Medicine and Biotechnology, PGIMER, Chandigarh, for providing the human breast cancer cell line, MDA-MB-231, for in vitro cell culture experiments.

REFERENCES

(1) Arruebo, M.; Vilaboa, N.; Sáez-Gutierrez, B.; Lambea, J.; Tres, A.; Valladares, M.; González-Fernández, Á. Assessment of the Evolution of Cancer Treatment Therapies. *Cancers* **2011**, *3*, 3279−3330.

(2) Wahajuddin; Arora, S. Superparamagnetic Iron Oxide Nanoparticles: Magnetic Nanoplatforms as Drug Carriers. *Int. J. Nanomed.* **2012**, *7*, 3445−3471.

(3) Koirala, N.; Das, D.; Fayazzadeh, E.; Sen, S.; McClain, A.; Puskas, J. E.; Drazba, J. A.; McLennan, G. Folic Acid Conjugated Polymeric Drug Delivery Vehicle for Targeted Cancer Detection in Hepatocellular Carcinoma. *J. Biomed. Mater. Res.* **2019**, *107*, 2522−2535.

(4) Law, S.; Leung, A. W.; Xu, C. Folic Acid-Modified Celastrol Nanoparticles: Synthesis, Characterization, Anticancer Activity in 2D and 3D Breast Cancer Models. *Artif. Cells Nanomed. Biotechnol.* **2020**, *48*, 542−559.

(5) DeCarlo, A.; Malardier-Jugroot, C.; Szewczuk, M. R. Folic Acid-Functionalized Nanomedicine: Folic Acid Conjugated Copolymer and Folate Receptor Interactions Disrupt Receptor Functionality Resulting in Dual Therapeutic Anti-Cancer Potential in Breast and Prostate Cancer. *Bioconjugate Chem.* **2021**, *32*, 512−522.

(6) Bhatia, S. Nanoparticles Types, Classification, Characterization, Fabrication Methods and Drug Delivery Applications. In *Natural Polymer Drug Delivery Systems Nanoparticles, Plants, and Algae*; Springer: Switzerland, 2016; pp 33−93.

(7) Senapati, S.; Mahanta, A. K.; Kumar, S.; Maiti, P. Controlled Drug Delivery Vehicles for Cancer Treatment and Their Performance. *Signal Transduction Targeted Ther.* **2018**, *3*, No. 7.

(8) Biabanikhankahdani, R.; Ho, K.; Alitheen, N.; Tan, W. A Dual Bioconjugated Virus-Like Nanoparticle as a Drug Delivery System and Comparison with a PH-Responsive Delivery System. *Nanomaterials* **2018**, *8*, No. 236.

(9) Zhang, Y.; Wu, X.; Han, Y.; Mo, F.; Duan, Y.; Li, S. Novel Thymopentin Release Systems Prepared from Bioresorbable PLA-PEG-PLA Hydrogels. *Int. J. Pharm.* **2010**, *386*, 15−22.

(10) Quesnel, R.; Hildgen, P. Synthesis of PLA-b-PEG Multiblock Copolymers for Stealth Drug Carrier Preparation. *Molecules* **2005**, *10*, 98−104.

(11) Cohn, D.; Younes, H. Biodegradable PEO/PLA Block Copolymers. *J. Biomed. Mater. Res.* **1988**, *22*, 993−1009.

(12) Hami, Z.; Amini, M.; Ghazi-Khansari, M.; Rezayat, S. M.; Gilani, K. Synthesis and in Vitro Evaluation of a PH-Sensitive PLA-PEG-Folate Based Polymeric Micelle for Controlled Delivery of Docetaxel. *Colloids Surf., B* **2014**, *116*, 309−317.

(13) Hami, Z.; Amini, M.; Ghazi-Khansari, M.; Rezayat, S. M.; Gilani, K. Doxorubicin-Conjugated PLA-PEG-Folate Based Polymeric

https://doi.org/10.1021/acsomega.1c06338
ACS Omega 2022, 7, 5231−5241

Micelle for Tumor-Targeted Delivery: Synthesis and in Vitro Evaluation. *DARU, J. Pharm. Sci.* **2014**, *22*, No. 30.
(14) Amani, A.; Kabiri, T.; Shafiee, S.; Hamidi, A. Preparation and Characterization of PLA-PEG-PLA/PEI/DNA Nanoparticles for Improvement of Transfection Efficiency and Controlled Release of DNA in Gene Delivery Systems. *Iran. J. Pharm. Res.* **2019**, *18*, 125−141.
(15) Andima, M.; Costabile, G.; Isert, L.; Ndakala, A.; Derese, S.; Merkel, O. M. Evaluation of β-Sitosterol Loaded PLGA and PEG-PLA Nanoparticles for Effective Treatment of Breast Cancer: Preparation, Physicochemical Characterization, and Antitumor Activity. *Pharmaceutics* **2018**, *10*, No. 232.
(16) Alyafee, Y. A.; Alaamery, M.; Bawazeer, S.; Almutairi, M. S.; Alghamdi, B.; Alomran, N.; Sheereen, A.; Daghestani, M.; Massadeh, S. Preparation of Anastrozole Loaded PEG-PLA Nanoparticles: Evaluation of Apoptotic Response of Breast Cancer Cell Lines. *Int. J. Nanomed.* **2018**, *13*, 199−208.
(17) Kumar, M.; Gupta, D.; Singh, G.; Sharma, S.; Bhat, M.; Prashant, C. K.; Dinda, A. K.; Kharbanda, S.; Kufe, D.; Singh, H. Novel Polymeric Nanoparticles for Intracellular Delivery of Peptide Cargos: Antitumor Efficacy of the BCL-2 Conversion Peptide NuBCP-9. *Cancer Res.* **2014**, *74*, 3271−3281.
(18) Gudiña, E. J.; Rangarajan, V.; Sen, R.; Rodrigues, L. R. Potential Therapeutic Applications of Biosurfactants. *Trends Pharmacol. Sci.* **2013**, *34*, 667−675.
(19) Rodrigues, L. R. Microbial Surfactants: Fundamentals and Applicability in the Formulation of Nano-Sized Drug Delivery Vectors. *J. Colloid Interface Sci.* **2015**, *449*, 304−316.
(20) Bansal, S.; Singh, J.; Kumari, U.; Kaur, I. P.; Barnwal, R. P.; Kumar, R.; Singh, S.; Singh, G.; Chatterjee, M. Development of Biosurfactant-Based Graphene Quantum Dot Conjugate as a Novel and Fluorescent Theranostic Tool for Cancer. *Int. J. Nanomed.* **2019**, *14*, 809−818.
(21) Duncan, R.; Vicent, M. J. Polymer Therapeutics-Prospects for 21st Century: The End of the Beginning. *Adv. Drug Delivery Rev.* **2013**, *65*, 60−70.
(22) Ghasemi, R.; Abdollahi, M.; Emamgholi Zadeh, E.; Khodabakhshi, K.; Badeli, A.; Bagheri, H.; Hosseinkhani, S. MPEG-PLA and PLA-PEG-PLA Nanoparticles as New Carriers for Delivery of Recombinant Human Growth Hormone (RhGH). *Sci. Rep.* **2018**, *8*, No. 9854.
(23) Garg, M.; Priyanka; Chatterjee, M. Isolation, Characterization and Antibacterial Effect of Biosurfactant from Candida Parapsilosis. *Biotechnol. Rep.* **2018**, *18*, No. e00251.
(24) Wu, X.; Li, S. Synthesis of Polylactide/Poly(Ethylene Glycol) Diblock Copolymers with Functional Endgroups. *Polym. Int.* **2012**, *62*, 1014−1021.
(25) Mccall, R. L.; Sirianni, R. W. PLGA Nanoparticles Formed by Single- or Double-Emulsion with Vitamin E- TPGS. *J. Vis. Exp.* **2013**, *82*, No. e51015.
(26) Huang, W.; Lang, Y.; Hakeem, A.; Lei, Y.; Gan, L.; Yang, X. Surfactin-Based Nanoparticles Loaded with Doxorubicin to Overcome Multidrug Resistance in Cancers. *Int. J. Nanomed.* **2018**, *13*, 1723−1736.
(27) Singh, N. A.; Mandal, A. K. A.; Khan, Z. A. Fabrication of PLA-PEG Nanoparticles as Delivery Systems for Improved Stability and Controlled Release of Catechin. *J. Nanomater.* **2017**, *2017*, No. 6907149.
(28) Mahalingam, M.; Krishnamoorthy, K. Fabrication, Physicochemical Characterization and Evaluation of in Vitro Anticancer Efficacy of a Novel PH Sensitive Polymeric Nanoparticles for Efficient Delivery of Hydrophobic Drug against Colon Cancer. *J. Appl. Pharm. Sci.* **2015**, *5*, 135−145.
(29) Gouda, R.; Baishya, H.; Zhao, Q. Application of Mathematical Models in Drug Release Kinetics of Carbidopa and Levodopa ER Tablets. *J. Dev. Drugs* **2017**, *6*, No. 2.
(30) Guo, M.; Que, C.; Wang, C.; Liu, X.; Yan, H.; Liu, K. Multifunctional Superparamagnetic Nanocarriers with Folate-Mediated and PH-Responsive Targeting Properties for Anticancer Drug Delivery. *Biomaterials* **2011**, *32*, 185−194.
(31) Danaei, M.; Dehghankhold, M.; Ataei, S.; Hasanzadeh Davarani, F.; Javanmard, R.; Dokhani, A.; Khorasani, S.; Mozafari, M. R. Impact of Particle Size and Polydispersity Index on the Clinical Applications of Lipidic Nanocarrier Systems. *Pharmaceutics* **2018**, *10*, No. 57.
(32) Costa, P.; Lobo, J. M. S. Modeling and Comparison of Dissolution Profiles. *Eur. J. Pharm. Sci.* **2001**, *13*, 123−133.
(33) Gao, Y.; Zuo, J.; Bou-Chacra, N.; Pinto, T. D. J. A.; Clas, S. D.; Walker, R. B.; Löbenberg, R. In Vitro Release Kinetics of Antituberculosis Drugs from Nanoparticles Assessed Using a Modified Dissolution Apparatus. *BioMed Res. Int.* **2013**, *2013*, No. 136590.
(34) Kumar, A.; Ahuja, M. Carboxymethyl Gum Kondagogu-Chitosan Polyelectrolyte Complex Nanoparticles: Preparation and Characterization. *Int. J. Biol. Macromol.* **2013**, *62*, 80−84.
(35) Rana, S.; Singh, J.; Wadhawan, A.; Khanna, A.; Singh, G.; Chatterjee, M. Evaluation of In Vivo Toxicity of Novel Biosurfactant from Candida Parapsilosis Loaded in PLA-PEG Polymeric Nanoparticles. *J. Pharm. Sci.* **2021**, *110*, 1727−1738.
(36) Dong, J.; Wang, K.; Sun, L.; Sun, B.; Yang, M.; Chen, H.; Wang, Y.; Sun, J.; Dong, L. Application of Graphene Quantum Dots for Simultaneous Fluorescence Imaging and Tumor-Targeted Drug Delivery. *Sens. Actuators, B* **2018**, *256*, 616−623.

https://doi.org/10.1021/acsomega.1c06338
ACS Omega 2022, 7, 5231−5241